Quantification of trabecular spatial orientation from low-resolution images

Lenaerts L. [1], Wirth A.J. [2], van Lenthe G.H. [1,2*]

[1] *Biomechanics Section, KU Leuven, Leuven, Belgium*

[2] *Institute for Biomechanics, ETH Zurich, Zurich, Switzerland*

*** Corresponding Author:**

G. Harry van Lenthe

Biomechanics Section

Celestijnenlaan 300C

3001 Leuven, Belgium

harry.vanlenthe@mech.kuleuven.be

Tel. +32 16 322595

Fax +32 16 328999

Quantification of trabecular spatial orientation from low-resolution images

No accepted methodology exists to assess trabecular bone orientation from clinical CT-scans. The aim of this study was to test the hypothesis that the distribution of gray values in clinical CT-images is related to the underlying trabecular architecture and that this distribution can be used to identify the principal directions and local anisotropy of trabecular bone.

Fourteen trabecular bone samples were extracted from high-resolution (30 micron) micro-CT-scans of 7 human femoral heads. Trabecular orientations and local anisotropy were calculated using Gray Level Deviation (GLD), a novel method providing a measure of the three-dimensional distribution of image gray values. This was repeated for different image resolutions down to 300 micron and for volumes of interest ranging from 1 mm to 7 mm. Outcomes were compared to the principal mechanical directions and to Mean Intercept Length (MIL) as calculated for the segmented 30 micron images.

For the 30 micron images GLD predicted the mechanical principal directions equally well as MIL. For the 300 micron images, which is a resolution that can be obtained in vivo using clinical CT, only a small increase (3 - 6 degrees) in the deviation from the mechanical orientations was found. VOIs of 5 mm resulted in a robust quantification of the orientation. We conclude that GLD can quantify structural bone parameters from low-resolution CT images.

Keywords: bone; anisotropy; mean intercept length; finite element analysis, gray level deviation

Introduction

Bone mineral density (BMD) as measured using dual-energy X-ray absorptiometry (DXA) is typically used in order to diagnose osteoporosis. Yet, bone density only explains around 70% of the variance in mechanical properties of bone (Goulet et al. 1994) and fracture risk (Roberts et al. 2010). The gold standard to quantify bone

mechanical properties is through mechanical testing. Obviously, this is not feasible when investigating bone structures in vivo. As an alternative, finite element (FE) analysis is commonly used to simulate these mechanical tests. Starting from *in vivo* computed tomography (CT) images, FE models can be built and mechanical tests can be simulated. Unlike BMD measurements, FE modeling does not only take into account bone mass but also structural parameters. It can combine bone mass, bone geometry and internal trabecular architecture into one model capable of predicting bone mechanical behavior (Lenaerts and van Lenthe 2009). Using such FE models, it has been shown that the combination of bone volume fraction, trabecular orientation and degree of anisotropy can explain up to 94% of the variance in the bone mechanical properties (Keaveny et al. 2001).

Most macroscopic bone models described in literature typically assume isotropic material properties (Keyak et al. 1990; Taddei et al. 2006), although it is known that cortical and trabecular bone exhibit orthotropic material behavior (Rho 1996; Yang et al. 1998). The anisotropic material properties of trabecular bone are directly related to its complex structure of plates and rods (Liu et al. 2008). Several image processing techniques have been developed to quantify these structural trabecular bone properties. Mean intercept length (MIL) method is the technique most frequently used, although other measures have been developed (Ketcham and Ryan 2004; Odgaard 1997). However, all these methods are only applicable on high-resolution images where individual trabeculae can be segmented from bone marrow. Current standard in vivo technology allows to obtain such images at peripheral sites like the forearm using high-resolution peripheral quantitative computed tomography (HR-pQCT). At other anatomical sites that are severely affected by osteoporosis like the hip and the spine, the

visualization of individual plates and rods is hampered by the limited resolution of the clinical CT-images (Gupta et al. 2008; Krug et al. 2010). Hence, binarization of these grayscale images leads to a severe loss of structural information.

We hypothesized that the distribution of gray values in these CT-images is related to the underlying trabecular architecture. Specifically, we hypothesized that this distribution can be used to identify the principal directions and local anisotropy of trabecular bone structures. It was the aim of this work to develop and validate a technique that can identify the principal directions and quantify local anisotropy of trabecular bone from clinical CT-scans.

Materials and Methods

Specimens

Fourteen cubic volumes of interest (VOI) with an edge length of 7 mm were selected from 7 μCT-scans (μCT80, Scanco Medical AG, Brüttisellen Switzerland) of resected femoral head specimens. The donors (5 female and 2 male) were between 56 and 79 years old (average = 67 year) and were diagnosed with coxarthrosis. The specimens were collected during orthopedic surgical interventions in the framework of building a human bone repository for future experimental work (ethics committee approval EK-29/27) (Wirth 2011). Image resolution was 30 μm (70 kV, 114 μA, 600 ms integration time, 0.18° rotation step). The μCT-images were filtered using a constrained three-dimensional Gaussian filter to partially suppress the noise in the volumes ($\sigma = 1.2$, support = 1). For each femoral head one VOI was selected from the metaphysis and one from the epiphysis.

GLD: Gray level deviation method

The original grayscale images of these volumes were used as input to a novel orientation detection method called gray level deviation (GLD). The GLD method is based on the line fraction deviation (LFD) method, which was originally developed to calculate structural orientations of square regions of interest in two-dimensional binary X-ray images (Geraets 1998) and later extended to calculate structural orientations of cubical VOIs in three-dimensional binary μCT images (Geraets et al. 2006; Geraets et al. 2008). The GLD method extends the LFD method by detecting the principal directions of the trabecular structure in volumetric data selected from a grayscale CT dataset. In order to do so, GLD defines a set of parallel lines which rotates around the centre of the VOI. The number of parallel lines depends on the size of the largest inscribed cubical volume in the VOI that can rotate around the VOI's center without intersecting the outer surface of the VOI and corresponds to *(number of voxels per edge length of inscribed cube)*^{2}. For 950 uniformly distributed orientations of this line set, the standard deviation (SD) of the mean gray values along the lines is calculated and presented in a three-dimensional polar plot (Figure 1). We assume that when the set of lines becomes more aligned with the principal direction of the structure, SD will become larger and the long axis of the resulting point cloud will indicate the main orientation of the investigated structure (Miller et al. 2002). An ellipsoid is fitted on the point cloud in order to define a second order fabric tensor (Cowin 1985). Subsequently, the three principal directions are determined by calculating the eigenvectors of this ellipsoid. The calculated eigenvectors correspond to the principal directions of the trabecular structure and the eigenvalues of the fabric tensor provide a measure for the local anisotropy.

A preliminary study of this method showed that the degree of anisotropy remains constant for volumes of interest equal or larger than 5 mm (Lenaerts et al. 2010).

Therefore, in this study GLD was applied to 5 mm VOI of which the centre coincides with the centre of the 7 mm VOI, selected in the original grayscale images. The calculated principal directions were expressed in the coordinate system defined by the mechanical principal directions, calculated as described in the next section and three orthogonal projections were made to visualize the results.

Principal mechanical directions

In order to calculate the principal mechanical directions using FE analysis (FEA), the data were binarized using a global threshold corresponding to 285.6 mg HA/cc. Since the resolution of the thresholded μCT-images is high, the extracted bone represented well the actual structure (Bouxsein et al. 2010). All gray values higher than the chosen threshold were set to a high CT value, all gray values lower than the threshold were set a low CT value. The finite element models of the 5 mm samples, as used by the GLD method, were built directly from these binary images of the VOI by converting each isotropic 30 μm voxel into an 8-node brick element. Elements corresponding with the low CT value voxels were defined as marrow elements (E = 1 Pa). Elements corresponding with the high CT value were defined as bone elements (E = 10 GPa). Six FE analyses were performed for each model: three uniaxial compression tests along the imaging axes and three shear tests. The results of these six analyses were used to build the overall anisotropic stiffness matrix. From this stiffness matrix the principal mechanical directions and the corresponding fabric tensor of the sample were calculated (van Rietbergen et al. 1996).

MIL: Mean Intercept Length method

The mean intercept length method (Harrigan and Mann 1984; Whitehouse 1974) calculates the mean distance between consecutive material intersections along a defined set of parallel lines over a range of orientations. In every position of the line set the mean distance is plotted as a radius in a three-dimensional polar plot. The eigenvectors and the fabric tensor calculated from the ellipsoid fitted onto the resulting point cloud, estimate the principal directions and the local anisotropy. In this study, the MIL method was applied to the binarized 30 µm data as used by the FEA method. The principal directions were expressed in the coordinate system defined by the mechanical principal directions and three orthogonal projections were made to visualize the results.

Effect of VOI

To test the influence of the VOI dimension on the results of the GLD method, the trabecular structural parameters were additionally calculated for the VOI of 1 mm, 2 mm, 3 mm, 4 mm, 6 mm and 7 mm, selected to test the effect of the VOI size. For these different sizes of the VOI, the average angular differences of the 14 samples between the three GLD calculated principal directions and the GLD and FEA principal directions of the VOI with an edge length of 5 mm as references were calculated.

Effect of resolution

In order to evaluate the effect of the spatial resolution of the grayscale images on the anisotropic material properties using GLD, voxels of the 5 mm VOI were coarsened to resolutions of 60 µm, 90 µm, 120 µm, 150 µm, 180 µm, 210 µm, 240 µm, 270 µm and

300 µm. For each of these resolutions the principal directions and the local anisotropy were calculated.

The components of all calculated fabric tensors were normalized so that $H_1+H_2+H_3=1$.

Statistical evaluation

All angular differences between the principal directions calculated using GLD and MIL and the principal mechanical directions were checked for normality. Afterwards, paired t-tests or related samples Wilcoxon signed rank tests were used to determine the predictive value of GLD and MIL calculated orientations for the mechanical principal directions. Linear regression was used to determine the association between the components of the fabric tensor of the three investigated methods. All statistical analyses were performed in SPSS (IBM Corporation, Armonk, NY).

Results

Comparison of the methods

The first principal direction as determined by GLD closely matched the first principal mechanical direction with an average angular difference of 3.55° (Figure 2). The distribution pattern of the second and third principal direction calculated using GLD were more or less identical, but displayed a less dense pattern as the first principal direction. Hence, they deviated more from the second and third principal mechanical direction, 13.08° and 13.02° respectively.

Comparison of the principal directions calculated using the GLD and the FEA method and the MIL and the FEA method (Table 1) showed only small average

differences between the first principal directions of all three methods. These average differences were larger and almost identical for the second and the third principal direction.

The components H_1 and H_2 of the fabric tensor of GLD and the mechanical tensor correlated well (H_1: $R^2 = 0.52$; H_2: $R^2 = 0.70$) (Figure 3). Correlation of H_3 of both tensors was low ($R^2 = 0.18$) due to the variation in the H_3 of the GLD tensor. All three components of the fabric tensor of MIL correlated well with the components of the mechanical fabric tensor (H_1: $R^2 = 0.87$; H_2: $R^2 = 0.77$; H_3: $R^2 = 0.63$).

GLD: Influence of the size of the VOI

For small VOIs, H_1 showed some variation, but for volumes with an edge length higher than or equal to 5 mm, H_1 became more or less constant (Figure 4). Calculations of the angle between the principal mechanical directions as calculated for VOIs of 5 mm and the GLD calculated principal directions for VOIs from 1 to 7 mm, show a similar trend (Figure 5). In addition, expressing the GLD calculated principal directions for VOI from 1 to 7 mm in the coordinate frame defined by the mechanical principal directions showed that the angular difference became more or less constant for VOI equal or higher than 5 mm. However, when the principal directions calculated using GLD for VOI of 4 and 6 mm were expressed in the coordinate frame of the GLD calculated principal directions for the 5 mm VOI, results showed that this variation of the size of the 5 mm VOI with 1 mm, can lead to an average change in calculated orientations of 3° for the first principal direction and 7° to 13° for the second and third principal direction.

GLD: Influence of the spatial resolution

Irrespective of resolution, the first principal direction as calculated by GLD closely matched the principal mechanical direction as calculated using FE models based on 30 μm images (Figure 5). For the coarsest resolution the estimates were only slightly worse than for the best resolution (Figure 6). Specifically, the average angle between the first principal direction and the first mechanical orientation increased significantly with less than 3° ($p = 0.02$) when increasing voxel size from 30 μm to 300 μm. The second and third principal directions showed a significant increase in the mean deviation of approximately 5° to 6° from the mechanical orientations calculated using FEA ($p = 0.04 - 0.05$). For all three principal directions SD from the average angular difference increased with increasing voxel size. With decreasing resolution, H_1 decreased from 0.435 ± 0.022 to 0.406 ± 0.025 for the 30 μm and 300 μm resolution, respectively. H_2 and H_3 on the other hand, increased from 0.314 ± 0.021 and 0.252 ± 0.015, respectively, to 0.327 ± 0.018 and 0.268 ± 0.017, respectively (Figure 7).

Discussion

To validate the GLD method, the orientations calculated for 14 samples were compared with the orientations as obtained using the mean intercept length (MIL) method and with the mechanical orientations as calculated from FE analyses. The structural orientation of the trabeculae are typically used as a proxy for the mechanical orientation of a bone specimen; hence, the mechanical principal axes served as the ground truth in quantifying trabecular orientation, and MIL and GLD were expressed in the coordinate frame defined by the mechanical principal directions. Results showed that GLD predicts the mechanical principal directions equally well as MIL for high-resolution micro-CT images. Due to the heterogeneity of the trabecular architecture, the dimensions of the volume of interest had a strong effect on the predicted orientations. Lowering image

quality to a resolution that can be obtained in vivo using clinical CT, resulted in only a limited increase in the deviation of the GLD calculated principal directions from the principal mechanical directions.

In this study we hypothesized that the distribution in gray value in clinical CT images can be used to identify structural trabecular bone parameters like principal directions and local anisotropy. This hypothesis was confirmed. The results of this study showed that GLD predicts the principal mechanical directions. GLD gave a good prediction of the first principal direction with an average angular difference of 3.5°. This appears better than MIL, which showed an average angular error of 4.2°. However, this difference was not significant. Differences of 13° were found for the second and third principal directions. These larger deviations reflect the mechanical characteristics of the trabecular bone specimens that tended towards transverse isotropy (Keaveny et al. 2001). These calculated deviations are larger than the deviations reported between FE analyses and MIL by Odgaard et al. (1997). They found average angular differences of 1.4° for the first principal direction (FPD), 3.8° for the second principal direction (SPD) and 3.8° for the third principal (TPD) (Odgaard et al. 1997). However, in that study the cubic samples with an edge length of 10 mm were harvested from a whale vertebral body. Due to the size of this vertebral body the architecture of the trabecular specimens was much more uniform and the prediction of mechanical orientations from MIL orientations became more accurate. In human bone specimens of this size, there will be a large architectural variation. This was demonstrated in the present study by varying the size of the volume of interest. With a VOI of 5 mm as a reference, a change in VOI of 1 mm led to an average variation in structural orientations of 3° for the first principal directions up to 13° for the second and the third principal directions. Hence, the size of

the VOI chosen will have a large influence on the results when the trabecular architecture is not uniform.

The angular difference between GLD calculated orientations and the principal mechanical directions became more or less constant for VOIs larger than or equal to 5 mm. In addition, also the first component of the fabric tensor H_1 became more or less constant for volumes larger than or equal to 5 mm. This is probably related to the fact that from 5 mm onwards the trabecular bone behaves as a continuum (Harrigan et al. 1988).

Decreasing the image resolution of the grayscale images from 30 µm to 300 µm showed only a small increase of the average angular differences between the three principal directions of GLD and the principal mechanical directions (FPD: 2.53°; SPD: 5.77°; TPD: 6.33°). These results show that the gray level deviation method is able to determine structural bone parameters from clinical CT images of all anatomical sites. In addition to bone mass, these parameters can explain more than 90% of the variance in mechanical properties of bone (Goulet et al. 1994; Keaveny et al. 2001). In the past, several image processing techniques (Geraets 1998; Geraets et al. 2006; Ketcham and Ryan 2004; Odgaard 1997) have been developed to calculate these structural parameters, making use of the clear distinction between bone and marrow. In vivo, this requirement for binary input images limits the application of these methods to HR-pQCT-scans of the distal radius and tibia. At other anatomical sites that are severely affected by osteoporosis like the proximal femur and the vertebrae, current technology only allows to obtain resolutions in the same range as or larger than the size of individual trabeculae (100-200 µm). Hence, binarization of these images will lead to a major loss in structural information. Gray level deviation overcomes this limitation.

This study had some limitations. First, the developed GLD method was validated for trabecular bone samples only. In a preliminary study (Lenaerts and van Lenthe 2009) we demonstrated that GLD can be used to identify cortical orientation, at least in two-dimensional sections. Second, we lowered the resolution of the μCT-images by coarsening of the voxels. Yet, it has been shown that coarsening of high-resolution images has less influence on measured and calculated bone parameters than scanning at low resolution (Lenaerts and van Lenthe 2009). Third, an ellipsoid was fitted to the GLD calculated point cloud. This suffices to describe orthotropic material properties (Cowin 1985), but this approach may induce a small angular mismatch for specific bone samples with material properties going beyond orthotropy (Geraets et al. 2008). Fourth, the GLD method was validated for medical images with isotropic voxels. However, often current CT-imaging methods have a high in-plane but a low cross-plane resolution. We expect that the overall accuracy of the GLD calculated principal directions from anisotropic CT-images will be dependent of the scanning direction. Since the lowering of the image resolution has only a small influence on the results of the first principal direction, a lower resolution in a plane parallel with this direction will have little effect. A high resolution in the plane of the second and third principal directions will preserve the accuracy of the calculated orientations.

In conclusion, we found that the gray level deviation method is a novel image processing technique capable of detecting structural orientations of trabecular bone for high-resolution images (30 μm) as well as for low-resolution grayscale images

(300µm). Hence, GLD makes it possible to calculate bone structural parameters from in vivo clinical CT-images.

Acknowledgement

For the finite element analyses we used the infrastructure of the VSC – Flemish Supercomputer Center, funded by the Hercules Foundation and the Flemish Government – department EWI.

References

Bouxsein ML, Boyd SK, Christiansen BA, Guldberg RE, Jepsen KJ, Muller R. 2010. Guidelines for assessment of bone microstructure in rodents using micro-computed tomography. J.Bone Miner.Res. 25(7):1468-1486

Cowin SC. 1985. The relationship between the elasticity tensor and the fabric tensor. Mech.Mater. 4137-147

Geraets WG. 1998. Comparison of two methods for measuring orientation. Bone. 23(4):383-388

Geraets WG, van Ruijven LJ, Verheij JG, van der Stelt PF, van Eijden TM. 2008. Spatial orientation in bone samples and Young's modulus. J.Biomech. 41(10):2206-2210

Geraets WG, van Ruijven LJ, Verheij JG, van Eijden TM, van der Stelt PF. 2006. A sensitive method for measuring spatial orientation in bone structures. Dentomaxillofac.Radiol. 35(5):319-325

Goulet RW, Goldstein SA, Ciarelli MJ, Kuhn JL, Brown MB, Feldkamp LA. 1994. The relationship between the structural and orthogonal compressive properties of trabecular bone. J.Biomech. 27(4):375-389

Gupta R, Cheung AC, Bartling SH, Lisauskas J, Grasruck M, Leidecker C, Schmidt B, Flohr T, Brady TJ. 2008. Flat-panel volume CT: fundamental principles, technology, and applications. Radiographics. 28(7):2009-2022

Harrigan TP, Jasty M, Mann RW, Harris WH. 1988. Limitations of the continuum assumption in cancellous bone. J.Biomech. 21(4):269-275

Harrigan TP and Mann RW. 1984. Characterization of microstructural anisotropy in orthotropic materials using a second rank tensor. Journal of material science. 19761-767

Keaveny TM, Morgan EF, Niebur GL, Yeh OC. 2001. Biomechanics of trabecular bone. Annu.Rev.Biomed.Eng. 3307-333

Ketcham RA and Ryan TM. 2004. Quantification and visualization of anisotropy in trabecular bone. J.Microsc. 213(Pt 2):158-171

Keyak JH, Meagher JM, Skinner HB, Mote CD, Jr. 1990. Automated three-dimensional finite element modelling of bone: a new method. J.Biomed.Eng. 12(5):389-397

Krug R, Burghardt AJ, Majumdar S, Link TM. 2010. High-resolution imaging techniques for the assessment of osteoporosis. Radiol.Clin.North Am. 48(3):601-621

Lenaerts L, Knippels I, Melton LJI, Khosla S, van Lenthe GH. 2010. Determining local anisotropy in clinical CT images using a new orientation detection method: Gray Level Deviation (GLD). Congress of the European Society of Biomechanics.Edinburgh, 5-8 July.

Lenaerts L and van Lenthe GH. 2009. Multi-level patient-specific modelling of the proximal femur. A promising tool to quantify the effect of osteoporosis treatment. Philos.Transact.A Math.Phys.Eng Sci. 367(1895):2079-2093

Liu XS, Sajda P, Saha PK, Wehrli FW, Bevill G, Keaveny TM, Guo XE. 2008. Complete volumetric decomposition of individual trabecular plates and rods and its morphological correlations with anisotropic elastic moduli in human trabecular bone. J.Bone Miner.Res. 23(2):223-235

Miller Z, Fuchs MB, Arcan M. 2002. Trabecular bone adaptation with an orthotropic material model. J.Biomech. 35(2):247-256

Odgaard A. 1997. Three-dimensional methods for quantification of cancellous bone architecture. Bone. 20(4):315-328

Odgaard A, Kabel J, van Rietbergen B, Dalstra M, Huiskes R. 1997. Fabric and elastic principal directions of cancellous bone are closely related. J.Biomech. 30(5):487-495

Rho JY. 1996. An ultrasonic method for measuring the elastic properties of human tibial cortical and cancellous bone. Ultrasonics. 34(8):777-783

Roberts BJ, Thrall E, Muller JA, Bouxsein ML. 2010. Comparison of hip fracture risk prediction by femoral aBMD to experimentally measured factor of risk. Bone. 46(3):742-746

Taddei F, Cristofolini L, Martelli S, Gill HS, Viceconti M. 2006. Subject-specific finite element models of long bones: An in vitro evaluation of the overall accuracy. J.Biomech. 39(13):2457-2467

van Rietbergen B, Odgaard A, Kabel J, Huiskes R. 1996. Direct mechanics assessment of elastic symmetries and properties of trabecular bone architecture. J.Biomech. 29(12):1653-1657

Whitehouse WJ. 1974. The quantitative morphology of anisotropic trabecular bone. J.Microsc. 101(Pt 2):153-168

Wirth AJ. 2011. Assessment of implant stability in low quality bone by micro-structural finite element analysis.

Yang G, Kabel J, van Rietbergen B, Odgaard A, Huiskes R, Cowin SC. 1998. The anisotropic Hooke's law for cancellous bone and wood. J.Elast. 53(2):125-146

Table 1. Average angle between the first, second, and third principal direction using the GLD and the FEA method and the MIL and the FEA method, respectively.

Figure 1: Graphical representation of the gray level deviation method (GLD): For each orientation of the line set, standard deviation of the mean gray values along the lines is calculated and presented in a three dimensional polar plot. The three principal directions and local anisotropy are determined by first fitting an ellipsoid on the point cloud and then calculating the eigenvectors and fabric tensor of this ellipsoid. The calculated eigenvectors correspond to the principal directions of the trabecular structure and the components of the fabric tensor give a measure for the local anisotropy.

Figure 2: Orthogonal projection of the principal directions of the gray level deviation (GLD) method (full circles) and the mean intercept length (MIL) method (circles) for 14 bone specimens. Results are plotted in the coordinate frame of the principal mechanical directions.

Figure 3: Components of the fabric tensor calculated using the gray level deviation (GLD) method (top) and the mean intercept length (MIL) method (bottom) versus the components of the fabric tensor of the principal mechanical directions for 14 bone specimens.

Figure 4: Evolution of the average normalized components of the fabric tensor for different sizes of the volume of interest (VOI) of 14 bone specimens investigated using the Grey Level Deviation (GLD) method (full line). The dashed lines indicate the standard deviations from the mean components.

Figure 5: Evolution of the average angle between the principal mechanical directions for VOIs of 5 mm and the GLD calculated principal directions for VOIs of 1 to 7 mm.

Figure 6: Average angle for 14 bone specimens (full line) between the first (a), second (b) and third (c) principal directions of the finite element analysis (FEA) method and the gray level deviation (GLD) method for different spatial resolutions of the used images. The dashed lines indicate the standard deviations from the mean.

Figure 7: Evolution of the average normalized components of the fabric tensor for different image resolutions of 14 bone specimens investigated using the Grey Level Deviation (GLD) method (full lines). The dashed lines indicate the standard deviations from the means.

Figure 8: Orthogonal projection of the principal directions calculated from 30 μm resolution images (full circles) and from 300 μm resolution images (circles) using the gray level deviation method (GLD) for 14 bone specimens. These directions are plotted in the coordinate system of the principal mechanical directions calculated using finite element analysis (FEA).

	Deviation (degrees) in principal direction		
	first	**second**	**third**
GLD - FEA	3.55° ± 1.86°	13.08° ± 8.19°	13.02° ± 8.14°
MIL - FEA	4.23° ± 1.46°	10.26° ± 9.21°	10.50° ± 9.14°

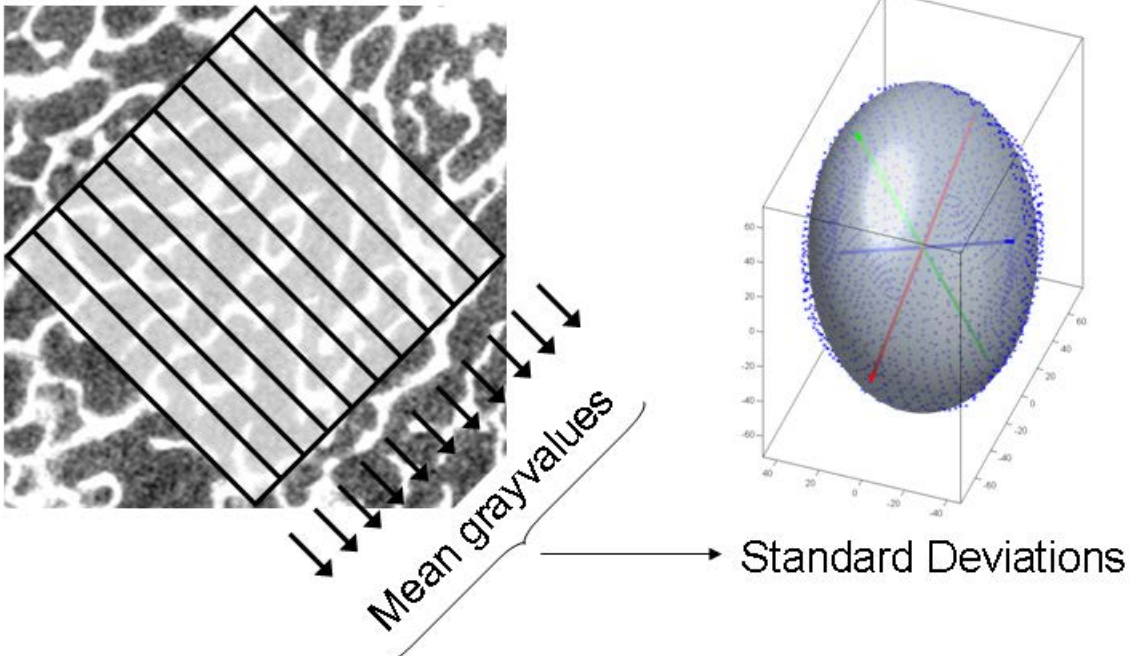
Mean grayvalues
Standard Deviations

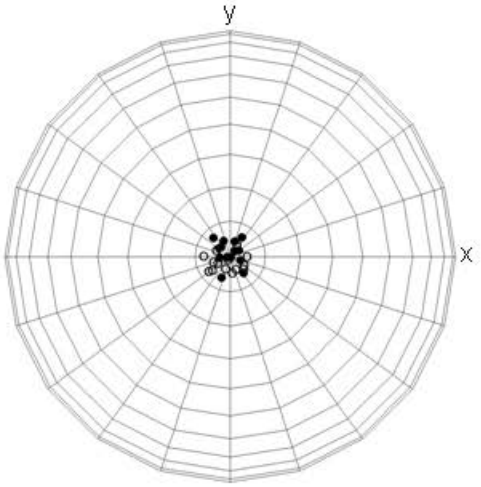

first principal direction

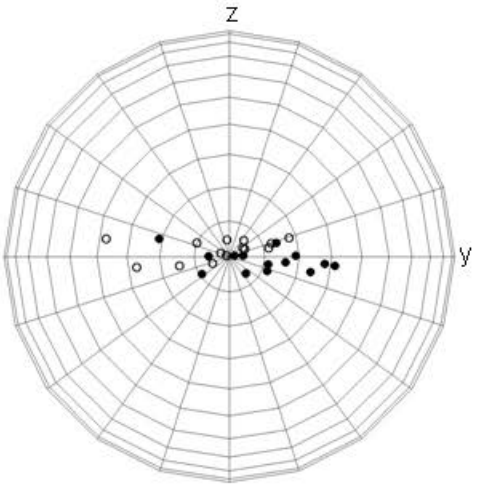

second principal direction

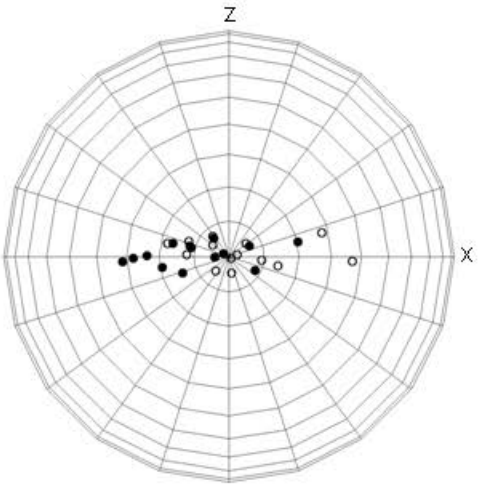

third principal direction

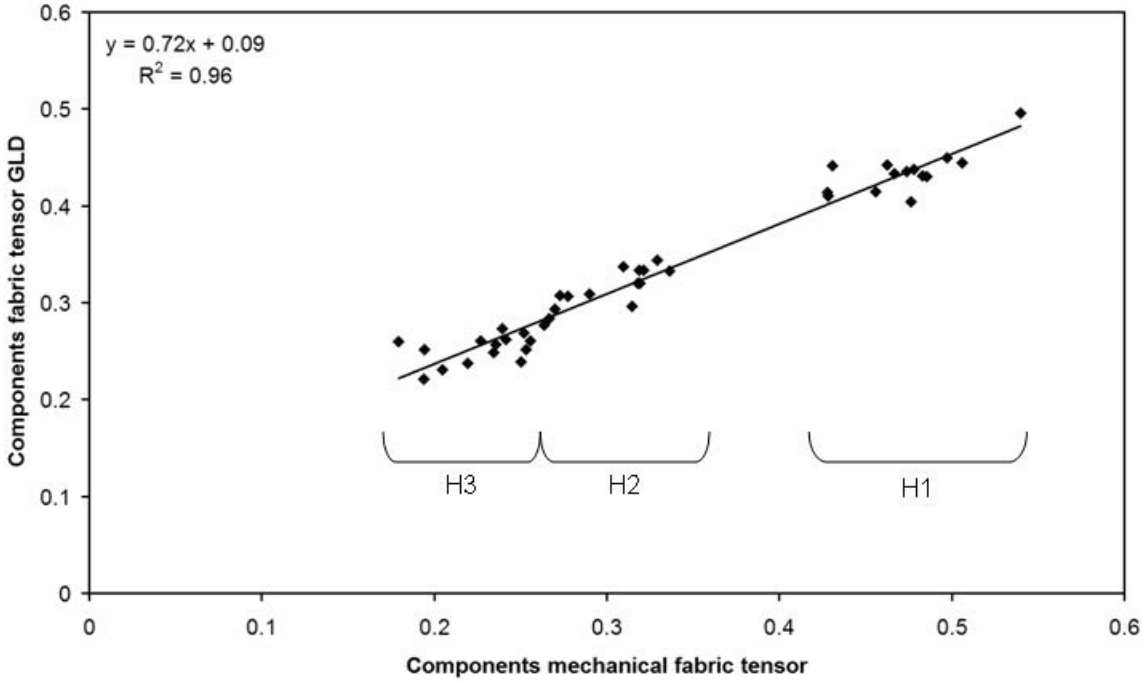
y = 0.72x + 0.09
R2 = 0.96
Components fabric tensor GLD
Components mechanical fabric tensor
H3
H2
H1
0
0.1
0.2
0.3
0.4
0.5
0.6

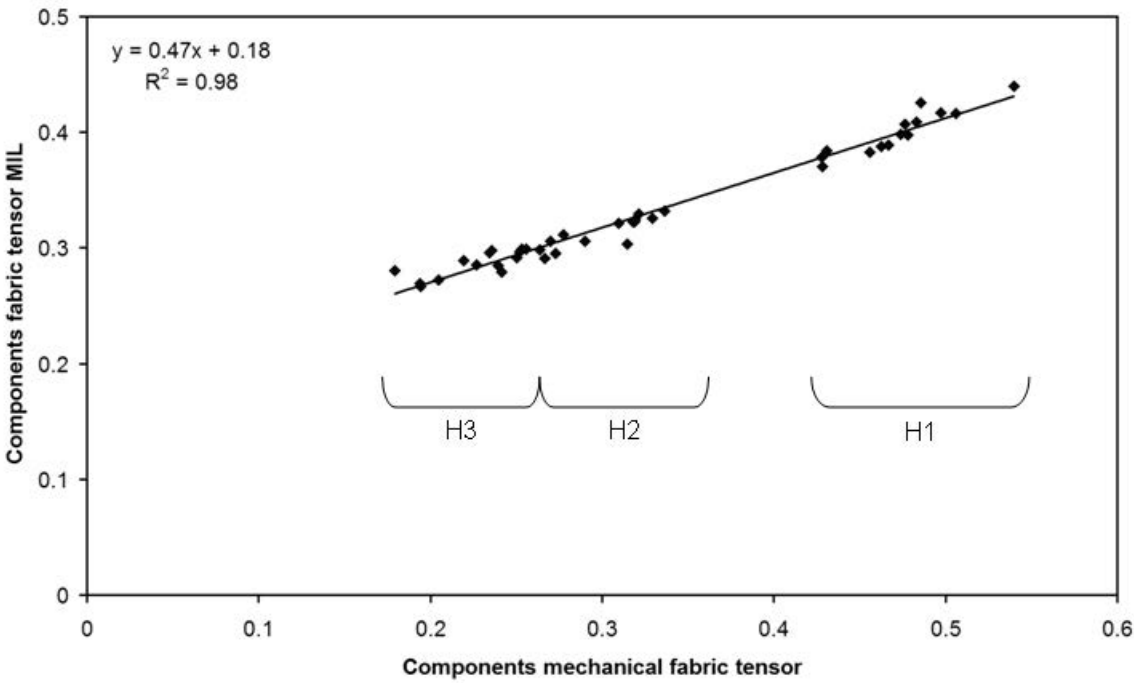
y = 0.47x + 0.18
R2 = 0.98
Components fabric tensor MIL
Components mechanical fabric tensor
H3
H2
H1
0
0.1
0.2
0.3
0.4
0.5
0.6

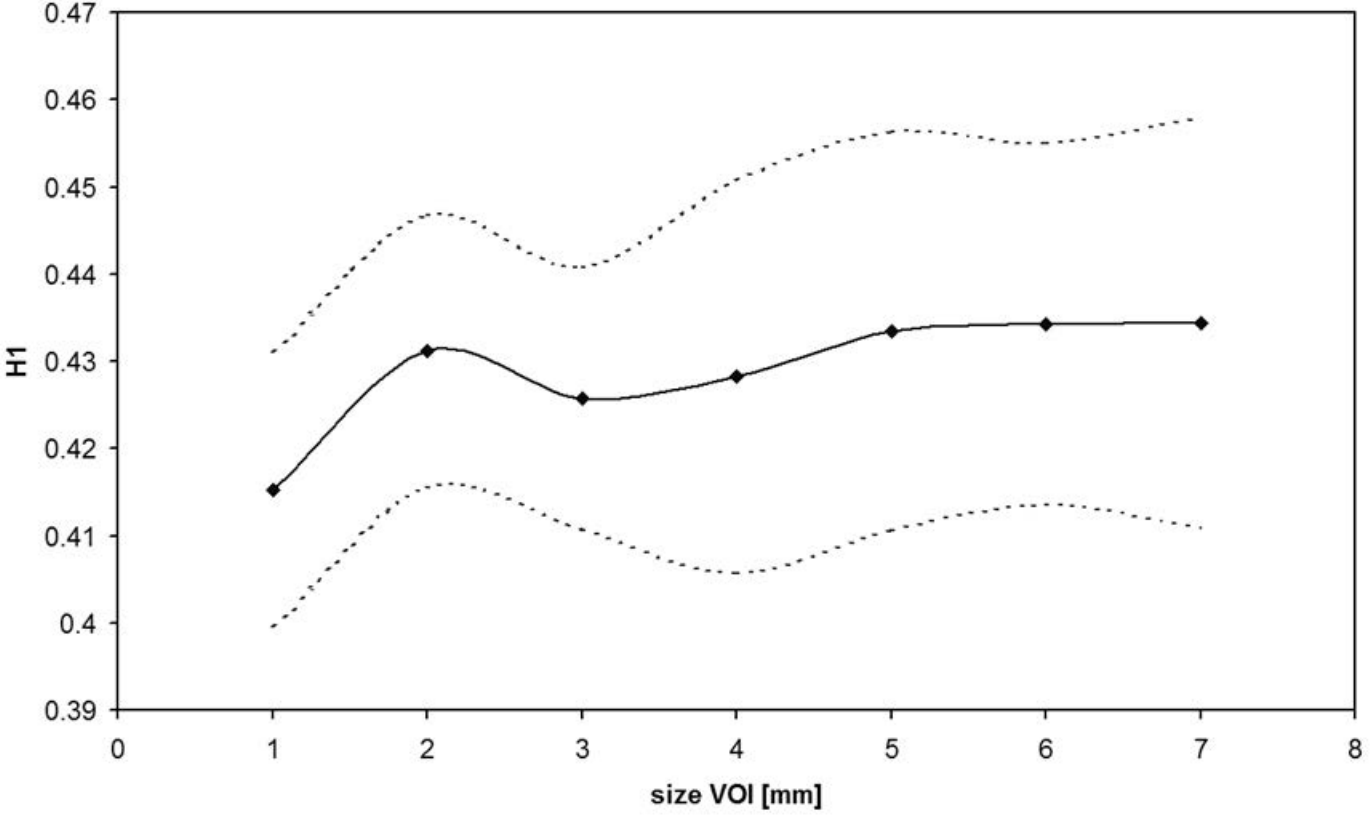
0.47
0.46
0.45
0.44
0.43
0.42
0.41
0.4
0.39
H1
0
1
2
3
4
5
6
7
8
size VOI [mm]

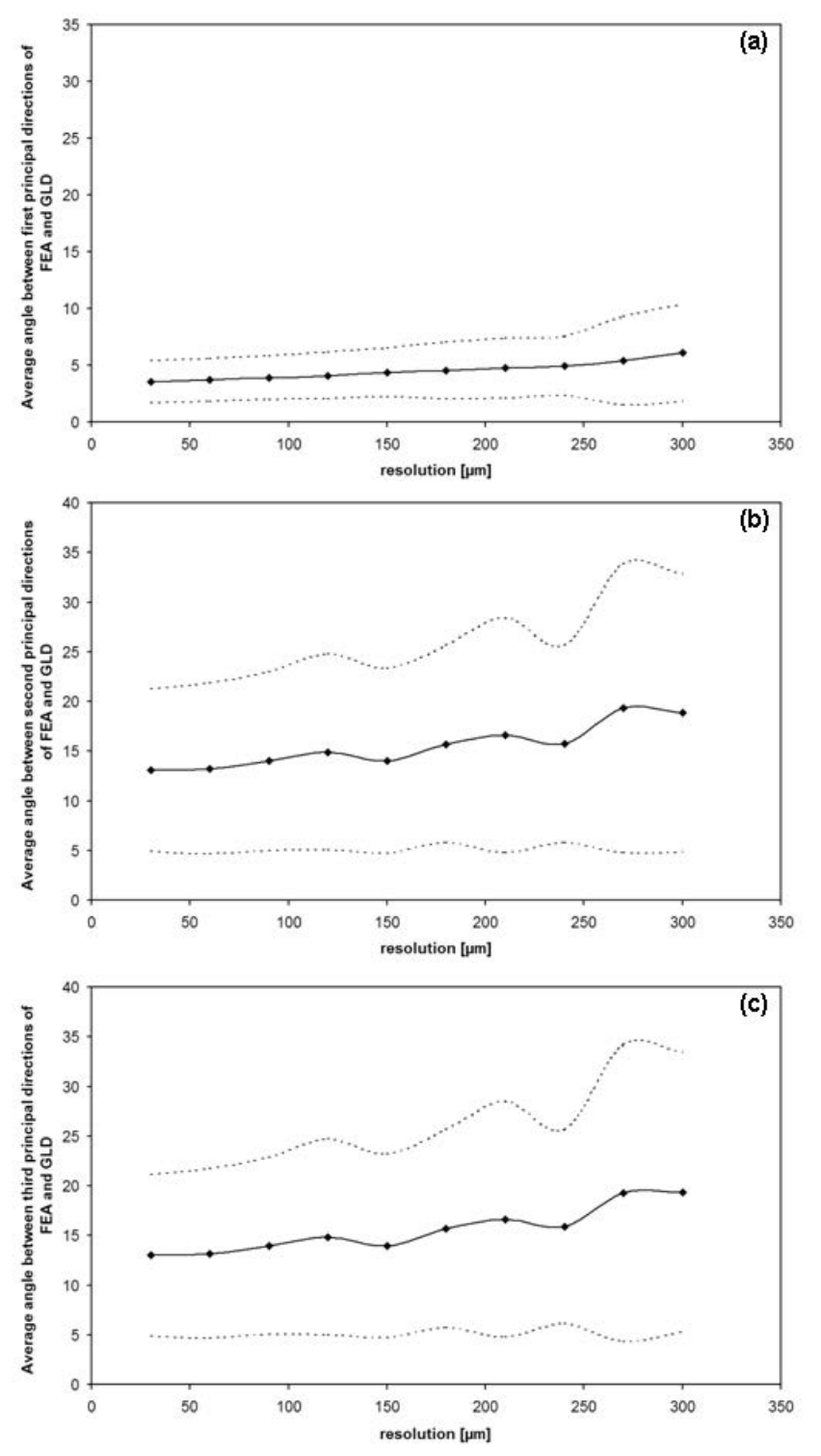
(a)
Average angle between first principal directions of FEA and GLD
resolution [µm]
(b)
Average angle between second principal directions of FEA and GLD
resolution [µm]
(c)
Average angle between third principal directions of FEA and GLD
resolution [µm]

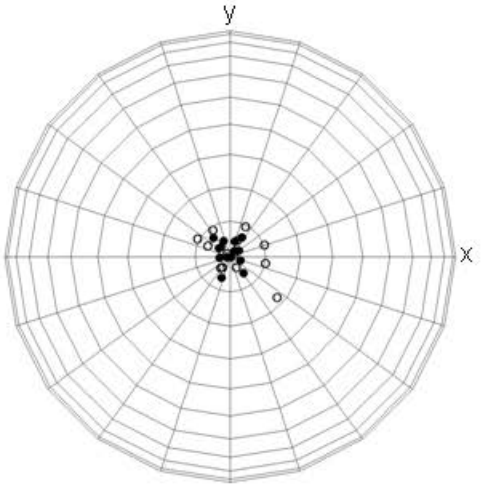

first principal direction

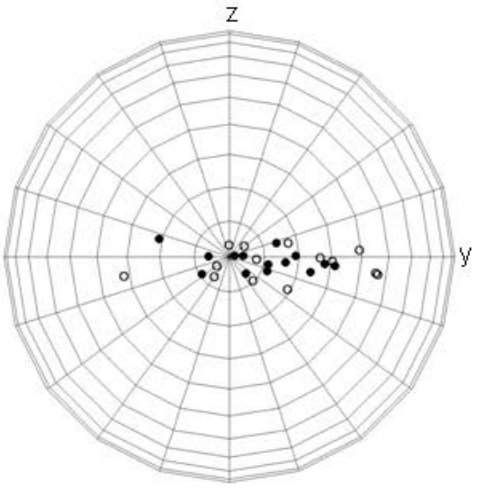

second principal direction

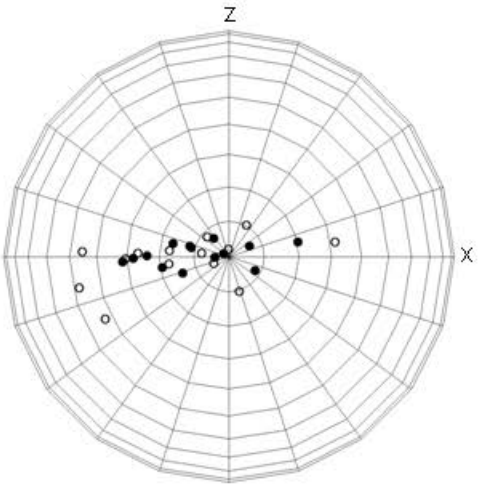

third principal direction